Preparation and Electrochemical Hydrogen Storage of Boron Nitride Nanotubes

X. Chen,[†] X. P. Gao,*[,†] H. Zhang,[†] Z. Zhou,[†] W. K. Hu,[†] G. L. Pan,[†] H. Y. Zhu,*[,‡] T. Y. Yan,[†] and D. Y. Song[†]

Institute of New Energy Material Chemistry, Department of Materials Chemistry, N & T Joint Academy, Nankai University, Tianjin 300071, China, and Australian Key Centre of Microanalysis & Microscopy and School of Chemistry, The University of Sydney, New South Wales 2006, Australia

Received: January 7, 2005; In Final Form: April 12, 2005

Boron nitride (BN) nanotubes were synthesized through chemical vapor deposition over a wafer made by a $LaNi_5$/B mixture and nickel powder at 1473 K. Scanning electron microscopy, transmission electron microscopy, energy-dispersive spectroscopy, X-ray diffraction, and X-ray photoelectron spectroscopy were performed to characterize the microstructure and composition of BN nanotubes. It was found that the obtained BN nanotubes were straight with a diameter of 30−50 nm and a length of up to several microns. We first verify that the BN nanotubes can storage hydrogen by means of an electrochemical method, though its capacity is low at present. The hydrogen desorption of nonelectrochemical recombination in cyclic voltammograms, which is considered as the slow reaction at BN nanotubes, suggests the possible existence of strong chemisorption of hydrogen, and it may lead to the lower discharge capacity of BN nanotubes. It is tentatively concluded that the improvement of the electrocatalytic activity by surface modification with metal or alloy would enhance the electrochemical hydrogen storage capacity of BN nanotubes.

I. Introduction

Boron nitride (BN) nanotubes have been attracted much attention in recent years due to their unique structures and semiconductive properties. Several methods have been developed to synthesize BN nanotubes, including arc discharge,[1] chemical vapor deposition (CVD),[2] laser ablation,[3] and reactive ball-milling,[4] similar to carbon nanotubes. The preparation of BN nanotubes with a high purity is more important for their potential application. The growth of BN nanotubes depends strongly upon the presence of catalysts and precursors. Metallic particles,[5−7] alloy catalysts,[8] and boron compound precursors[9,10] were found to be very effective for the production of BN nanotubes. It was demonstrated that rare-earth-based AB_5 and Zr-based AB_2 hydrogen storage alloys, which are extensively used in metal hydride−nickel (MH/Ni) batteries, are good catalysts for the synthesis of carbon nanotubes.[11,12] Therefore, the utilization of the hydrogen storage alloy (for example, $LaNi_5$ alloy) as the catalyst precursor would be feasible and economical as compared with the LaB_6 alloy and metallic particles in the synthesis of BN nanotubes.

Hydrogen storage is a vital issue in the application of hydrogen as a future energy carrier. Many alloys are capable of reversibly storing large amounts of hydrogen, either through absorbing gaseous hydrogen at certain pressures and temperatures or by an electrochemical process to form a metal hydride.[13] However, traditional metal hydrides usually have the problems of low gravimetric storage capacities, and thus are not able to satisfy the requirements for practical hydrogen storage. In recent years, nonmetallic nanotube materials such as carbon nanotubes and BN nanotubes have attracted much attention as candidates for high hydrogen storage capacities.[14−18] It has been reported recently that BN nanotubes can uptake 1.8−2.6 wt % hydrogen under ∼10 MPa at room temperature[17] and collapsed BN nanotubes exhibit an even higher hydrogen adsorption capacity (4.2 wt %) than any multiwalled carbon nanotubes.[18] Theoretical calculations have also been performed to investigate hydrogen adsorption on BN nanotube and other fullerene materials.[19,20] It was suggested that the large uptake of hydrogen in BN nanotubes was primarily due to chemisorption.[6] In addition to the gas-phase reaction, hydrogen can also be stored in nanostructured carbon through electrochemical processes in aqueous solutions (KOH or H_2SO_4 electrolyte) under moderate conditions.[21−27] Therefore, hydrogen storage in BN nanotubes is also worth exploring through electrochemical processes.

In the present study, an effective method to synthesize large-scale BN nanotubes and control their morphologies was described using a $LaNi_5$ alloy as a catalyst precursor through chemical vapor deposition, and hydrogen storage of the BN nanotubes was also investigated in an electrochemical process. It was found for the first time that BN nanotubes can store hydrogen electrochemically, and such a study can also provide a further understanding of the mechanism of hydrogen storage in BN nanotubes through a gas-phase reaction.

II. Experimental Section

A. Sample Preparation and Characterization. The $LaNi_5$ hydrogen storage alloy powder and amorphous boron were mixed by ball-milling for 5 h with the mass ratio of 1:4. The mixture of 50 mg of the as-prepared $LaNi_5$/B and 150 mg of the Ni powder was pressed into a wafer under a pressure of 30 MPa. The wafer located in a ceramic boat was heated to 1473 K in a resistance furnace, while the argon gas passed through the quartz tubes during the process. Then ammonia gas was introduced to the above reaction system at a flow rate of 100 sccm for 1 h. After the reaction was completed, the wafer was dispersed ultrasonically in ethanol, and a drop in the above layer

* Authors to whom correspondence should be addressed. E-mail: xpgao@nankai.edu.cn; h.zhu@emu.usyd.edu.au.
[†] Nankai University.
[‡] The University of Sydney.

10.1021/jp050105u CCC: $30.25
Published on Web 05/19/2005

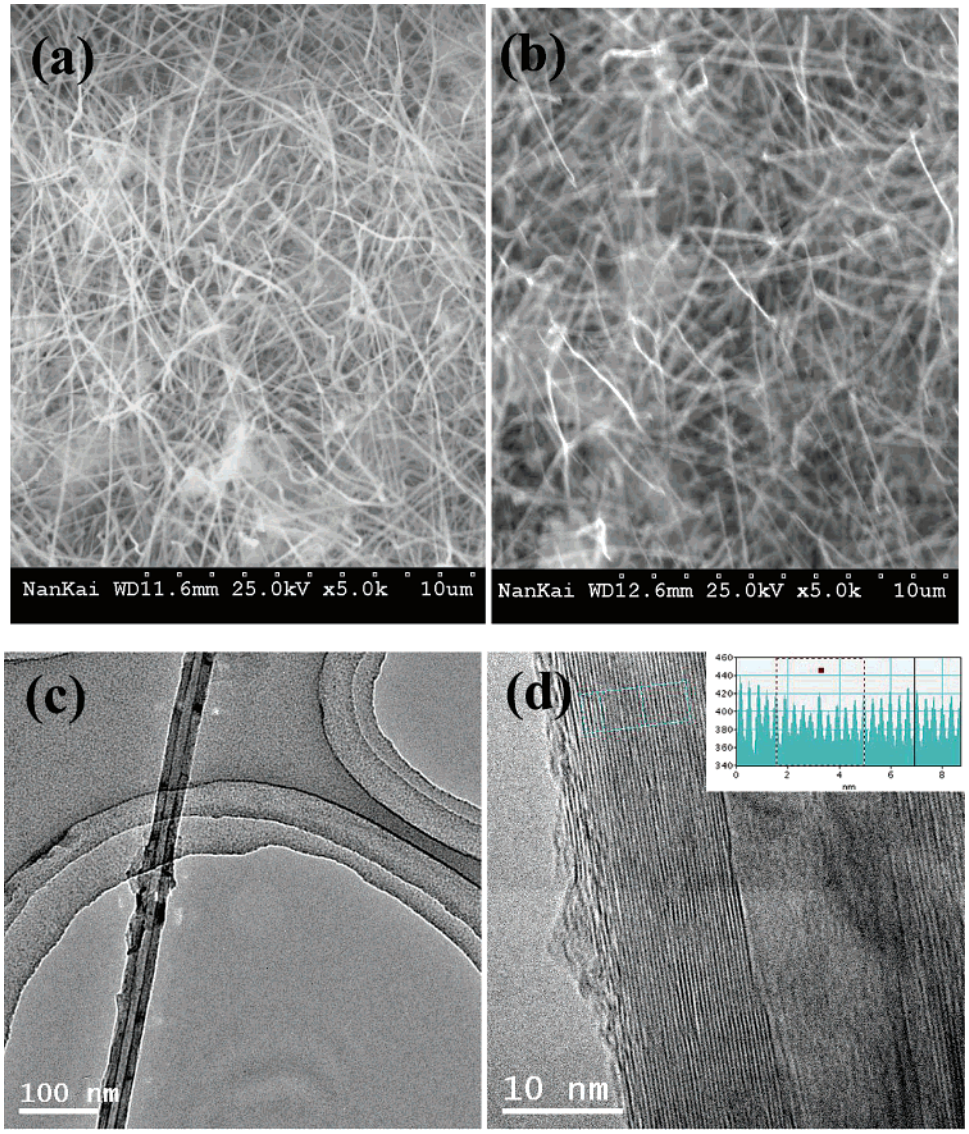

Figure 1. SEM images of the as-prepared wafer containing (a) dense BN nanotubes and (b) purified BN nanotubes and (c) TEM and (d) HRTEM images of an individual BN nanotube.

was placed on a copper grid. Scanning electron microscopy (SEM, Hitachi S-3500N), transmission electron microscopy (TEM, Tecnai 20), and X-ray photoelectron spectroscoy (XPS, PHI-5300ESCA) were employed to characterize the as-prepared samples.

B. Electrochemical Hydrogen Storage. The powder obtained on the surface of the as-prepared wafer was immersed in concentrated nitric acid for more than 24 h for purification and then washed with distilled water until pH = 7. The purified BN nanotubes (10 mg) and carbonyl nickel powders (INCO 255, 100 mg) were mixed completely and then pasted into the substrate of porous nickel. After being pressed, the above BN nanotube electrodes were applied to charge and discharge measurements. Electrochemical measurements of BN nanotube electrodes were performed in a three-electrode compartment using a sintered nickel electrode as the counter electrode and an Hg/HgO electrode as a reference electrode in 6 mol/L KOH electrolyte at room temperature in air (normal atmosphere). For comparison, the electrodes with commercial BN powders (hexagonal structure) were also prepared and measured under the same conditions as the blank. The working electrodes were fully charged at 500 or 1000 mA g^{-1} for 1 h and discharged at the same current density after a rest of 5 min in both charge/discharge curve and cycle life measurements. The discharge cutoff potential was set to be −0.4 V vs a Hg/HgO reference electrode. The cyclic voltammetric (CV) experiments were taken at different scan rates after fully charging using an IM6e electrochemical workstation (ZAHNER). The working electrodes for the CV experiments were prepared using the same method described above, except that the apparent surface of the porous nickel substrate was about 1.0 cm^2 and the carbonyl nickel powder was not added.

III. Results and Discussion

The as-prepared and purified BN nanotubes are up to several tens of microns long and 30−50 nm in diameter as shown in Figure 1. The tubes have a perfect multiwalled cylindrical structure and do not contain internal caps. The inner diameter of the BN nanotubes is almost uniform, approximately 6−10 nm. In Figure 2a, the strongest diffraction peaks of the purified BN nanotubes correspond to the (002) and (100) planes of BN compounds with a hexagonal structure (Joint Committee on Powder Diffraction Standards Card No. 34-0421), respectively. There are no impurities that can be detected from the X-ray diffraction (XRD) pattern, indicating that all of the catalysts and precursors can be removed during the purification. The

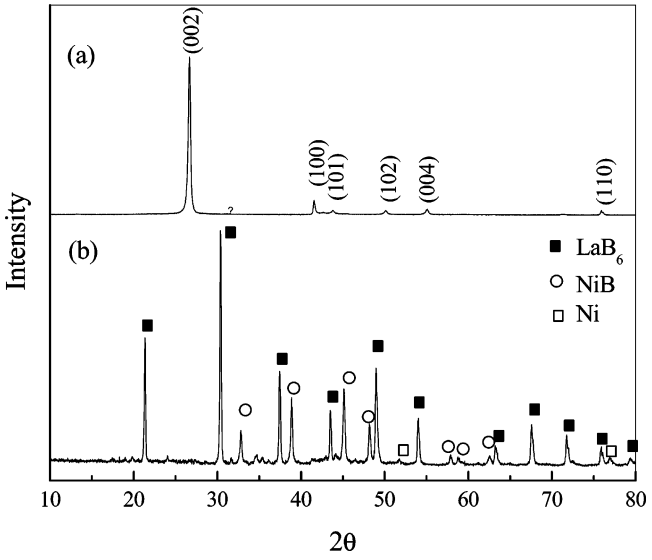

Figure 2. (a) XRD patterns of the purified BN nanotubes and (b) the calcined products of a $LaNi_5$ alloy and B powders mixed with nickel powders.

calculated interference fringe spacing is about 0.34 nm from the high-resolution TEM (HRTEM) image in Figure 1c, which corresponds to the (002) plane of the purified BN nanotubes and is in good agreement with the value derived from the XRD data. It is demonstrated from B_{1s} and N_{1s} core level XPS spectra of the purified products (Figure 3) that distinct peaks are observed at binding energies of 190 and 398 eV, respectively, revealing the existence of the BN compound. The atomic ratio of B to N was determined to be 0.97, which is close to the stoichiometric BN composition.[2,9] It is also confirmed by energy-dispersive specrometry (EDS, Figure 4) that there are not any impurities, indicating that La−Ni, Ni−B, and La−B alloys and metallic Ni are completely removed during purification. The Cu and C signals come from the Cu grid and the carbon film supporting the specimen in the TEM observation.

It can be seen from the XRD patterns of the calcined products of the $LaNi_5$ alloy and the B powders mixed with nickel powder that LaB_6, NiB, and a small amount of the residual Ni phases can be detected (Figure 2b). It is considered that boron reacted with $LaNi_5$ and Ni to form LaB_6 and NiB during the heat treatment process at the first stage. When the temperature is controlled to 1473 K and ammonia gas is introduced, BN is then synthesized by the reaction of superfluous boron and ammonia over NiB/LaB_6 particles. As for the growth mechanism of BN nanotubes, the chemical reactions in the whole process can be written as

$$LaNi_5(s) + Ni(s) + B(s) \rightarrow LaB_6(s) + NiB(s,l)$$

$$B(s) + NH_3(g) \xrightarrow{NiB(l)/LaB_6(s)} BN(s) + H_2(g)$$

The formation of liquid NiB here is a key catalyst for the second reaction.[28] It is observed from a SEM image that few BN nanotubes can be formed if only $LaNi_5$/B particles are performed. Once the nickel reagent is added with a suitable amount of boron powders, the NiB yield increases obviously. Moreover, the morphology of the BN nanotubes can be improved greatly. BN nanotubes are formed by the reaction of boron and ammonia gas in the liquid NiB droplet, which can be supported by previous literature.[28] And there is no evidence to suggest that LaB_6 is used as catalyst by the CVD method to produce BN nanotubes, but it probably prevents the NiB particles from agglomerating and keeps the melting point low of small-sized NiB particles. $LaNi_5$ alloy used here is more effective to form NiB intermetallic compounds for the subsequent synthesis of BN nanotubes.

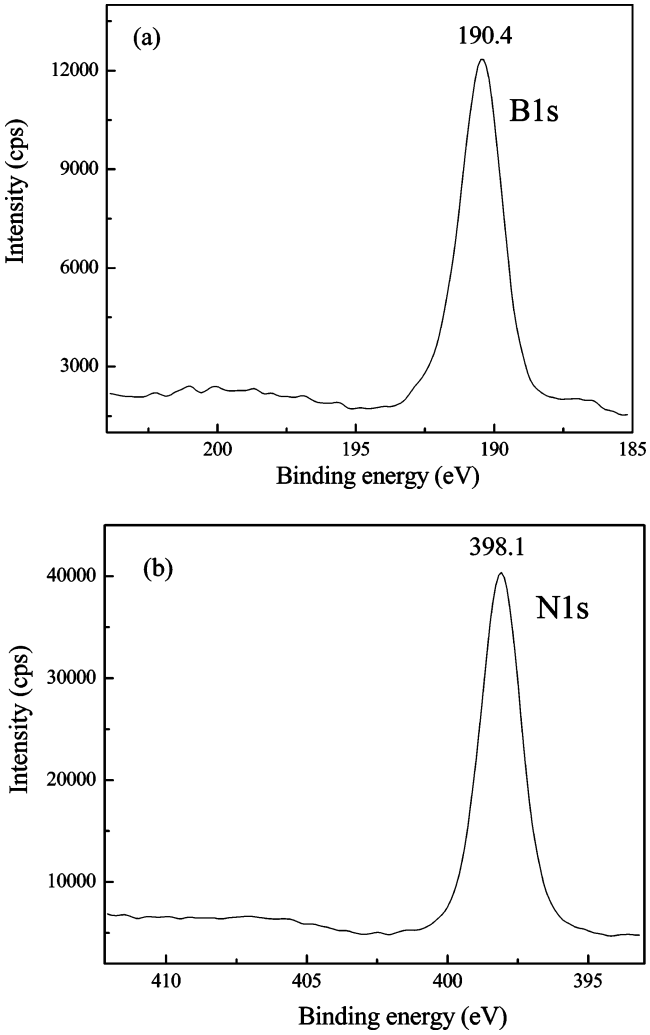

Figure 3. (a) B_{1s} and (b) N_{1s} core level spectra of the purified BN nanotubes.

To examine hydrogen storage in the electrochemical process, the first charge and discharge curves are shown in Figure 5a for the purified BN nanotube electrodes at different current densities. The initial electrochemical discharge capacities of 68 mA h g^{-1} (corresponding to ∼0.25 wt % hydrogen) and 54 mA h g^{-1} were obtained in the BN nanotube electrodes at the discharge current densities of 500 and 1000 mA g^{-1}, respectively. The discharge capacity of carbonyl nickel powders (INCO 255) is only 0.4 mA h g^{-1} as reported previously,[29] inferring that carbonyl nickel powders give a little contribution to the BN nanotube electrodes. In the meantime, for comparison, another electrode was prepared with commercial BN (hexagonal structure) powder as the blank electrode, and its discharge capacity was only 16 mA h g^{-1}, so the nanotubes have much higher electrochemical activities. It should be noted that the electrochemical hydrogen storage capacity obtained in this investigation is much lower than the hydrogen storage capacity reported in gas-phase reaction under a high pressure of 10 MPa or above.[17,18] The lower discharge capacity of the BN nanotubes may result from the normal atmosphere of 0.1 MPa (from the steady-state potential of −0.93 V vs a Hg/HgO reference electrode according to Nernst equation in 6 mol/L KOH solution at room temperature) in the electrochemical process. The cycle

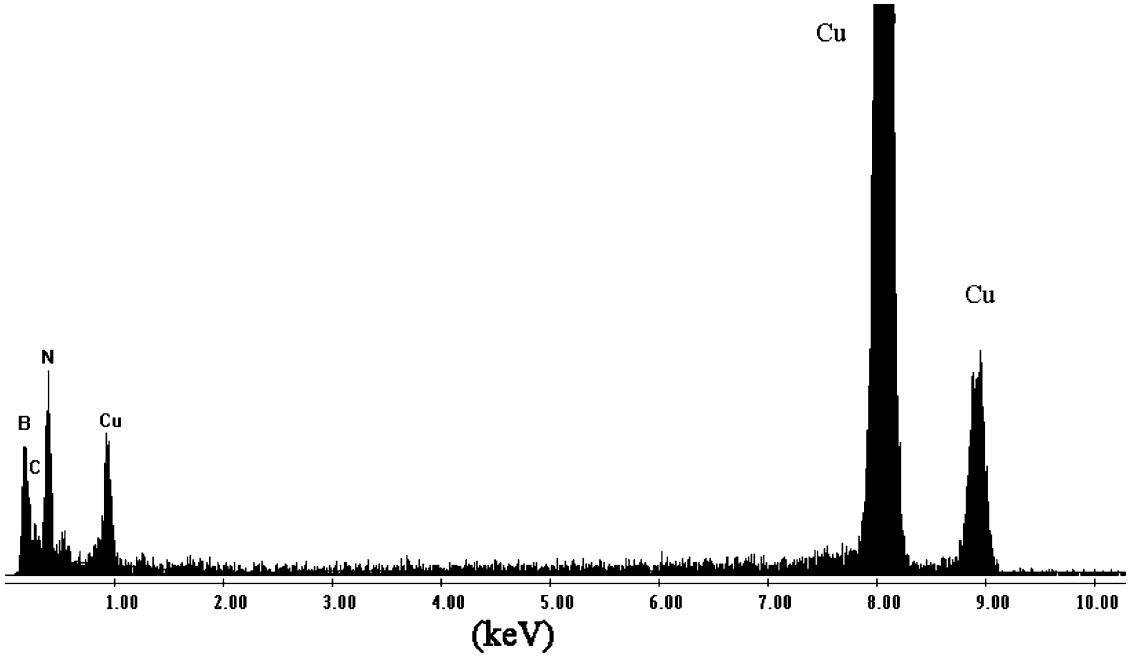

Figure 4. EDS spectrum of the purified BN nanotubes.

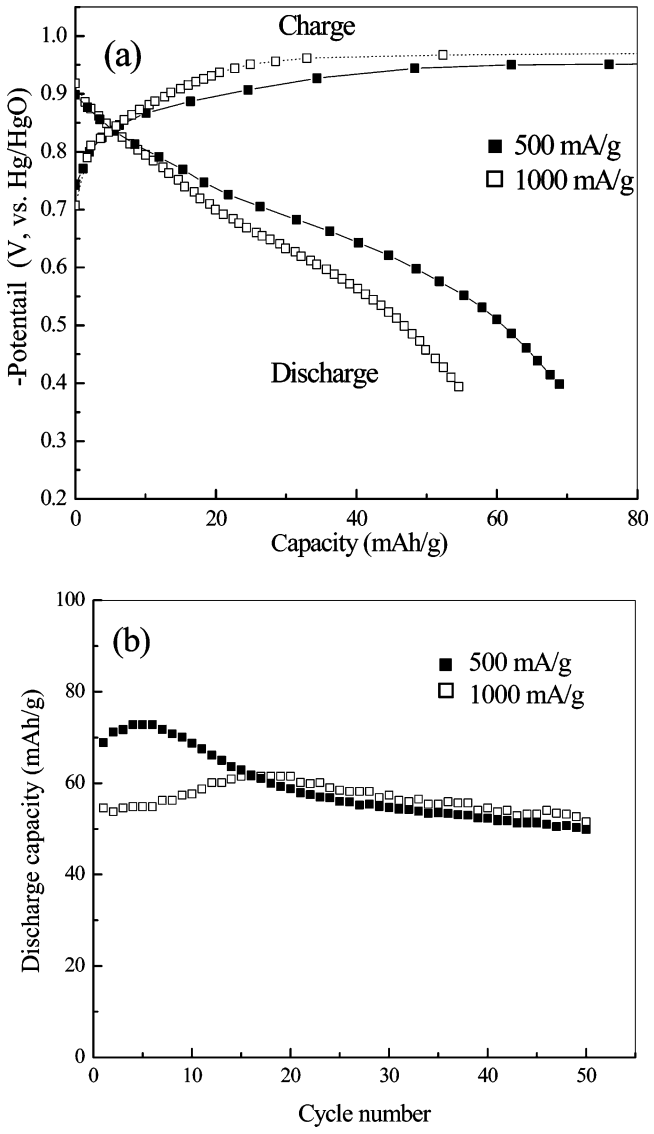

Figure 5. (a) First charge/discharge curves and (b) cycle life of purified BN nanotube electrodes at different current densities.

life of the purified BN nanotube electrodes at two current densities is shown in Figure 5b. A longer activation period was needed at the higher current density. The discharge capacities remain over 50 mA h g^{-1} after 50 cycles at the discharge current densities of 500 and 1000 mA g^{-1}. This suggests that the BN nanotubes have a strong resistance against oxidation and corrosion.

Cyclic voltammograms (CVs) were carried out to further examine the electrochemical hydrogen adsorption−oxidation reactions of purified BN nanotubes. As shown in Figure 6, the anodic oxidation peaks of hydrogen in the CVs are in the potential range between −0.50 and −0.55 V vs Hg/HgO, and the cathodic adsorption peaks of hydrogen are observed around −0.96 V, which is close to that of metal hydride electrodes and carbon nanotube electrodes.[22,30] Interestingly, the desorption peaks of hydrogen appear in the range between −0.78 and −0.85 V (depending on the scan rates) in the anodic process, indicating a slow desorption process of hydrogen at BN nanotubes. The electrochemical oxidation of hydrogen in the anodic process is dominant as usually observed in the CVs of metal hydride electrodes. Clearly, the desorption peak of hydrogen appears prior to the electrochemical oxidation peak of hydrogen, suggesting the possible existence of the strong chemisorption of hydrogen. The chemisorption was also found in the gas-phase reaction[17,18] and verified by theoretical calculation.[31] The mechanism of the electrochemical hydrogen storage process can be summarized as follows

$$BN + H_2O + e^- \leftrightarrow BN{-}H_{ads} + OH^-$$

$$BN{-}H_{ads} \leftrightarrow BN{-}H_{abs}$$

$$2BN{-}H_{ads} \Rightarrow 2BN + H_2$$

$BN{-}H_{ads}$ and $BN{-}H_{abs}$ are denoted as adsorbed hydrogen and absorbed hydrogen on BN nanotubes, respectively. Generally, a pair of adsorption and desorption peaks of hydrogen in the electrochemical reaction in the acidic media can be observed in Pd or Pd alloy electrodes due to the strong interaction of hydrogen with Pd.[32,33] Hydrogen desorption from the Pd

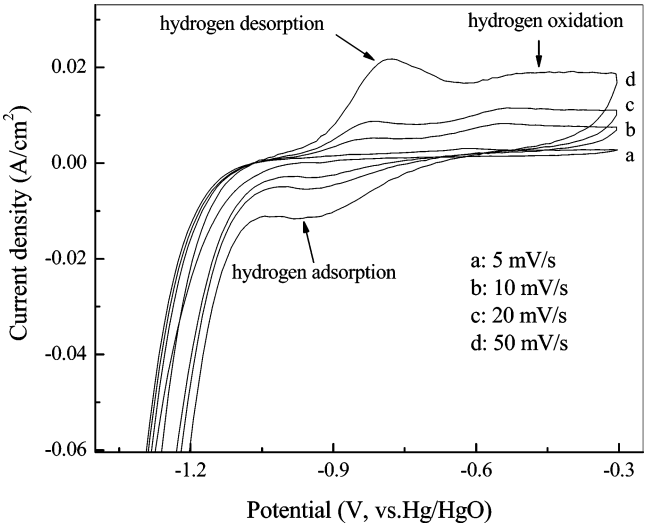

Figure 6. Cyclic voltammograms of the purified BN nanotube electrode at different scan rates. To avoid the perturbation of hydrogen adsorption of the metallic Ni powders, the electrodes used here were constructed only with porous Ni substrate and without the addition of carbonyl Ni powders.

electrode takes place in two mechanisms, electrochemical oxidation and nonelectrochemical recombination. However, in alkaline solution hydrogen desorption by nonelectrochemical recombination is seldom observed in metal hydride electrodes.[30] The Heyrovsky electrochemical oxidation process is dominant because of the high electrocatalytic activity of metal hydride electrodes. It is well-known that the electrocatalytic activity of nonmetallic BN compounds in alkaline solution is relatively poor, compared with that of metal hydride electrodes. The strong hydrogen desorption of nonelectrochemical recombination without charge transfer may lead to the low discharge capacity of BN nanotubes. The improvement of the electrocatalytic activity by surface modification with metals or alloys is expected to enhance the electrochemical hydrogen storage capacity of BN nanotubes, because it has been found that carbon nanotubes decorated with metallic Ni or Pd as catalysts showed a higher hydrogen storage capacity in the electrochemical and gas-phase reactions.[34−35]

IV. Conclusion

BN nanotubes were synthesized through chemical vapor deposition using a $LaNi_5$ alloy as a catalyst precursor at 1473 K. It was found that the obtained BN nanotubes are straight with a diameter of 30−50 nm and a length of up to several microns and can store hydrogen in an electrochemical process. An initial electrochemical discharge capacity of 68 mA h g^{-1} was obtained in the BN nanotube electrode. The anodic oxidation peak and cathodic adsorption peak of hydrogen were found in the cyclic voltammograms. The hydrogen desorption peak of nonelectrochemical recombination appeared at the range between −0.78 and −0.85 V, which is attributed to the slow reaction at BN nanotubes. The results reported here also suggest the possible existence of the strong chemisorption of hydrogen, and it may lead to the low discharge capacity of BN nanotubes. It is tentatively concluded that the improvement of the electrocatalytic activity by surface modification with metals or alloys would enhance the electrochemical hydrogen storage capacity of BN nanotubes.

Acknowledgment. This work was supported by the 973 Program (2002CB211800), NCET (040219), NSFC (50381037), TNSF (033804411), and CEM foundation for the N & T Joint Academy, China. Financial support from the Australian Research Council (ARC) is also gratefully acknowledged, and H. Y. Zhu is indebted to the ARC for a QE II fellowship.

References and Notes

(1) Chopra, N. G.; Luyren, R. J.; Cherry, K.; Crespi, V. H.; Cohen, M. L.; Louie, S. G.; Zettl, A. *Science* **1995**, *269*, 966.

(2) Lourie, O. R.; Jones, C. R.; Bartlett, B. M.; Gibbons, P. C.; Ruoff, R. S.; Buhro, W. E. *Chem. Mater.* **2000**, *12*, 1808

(3) Laude, T.; Matsui, Y.; Marraud, A.; Jouffrey, B. *Appl. Phys. Lett.* **2000**, *76*, 3239.

(4) Chen, Y.; Gerald, J. F.; Willams, J. S.; Bulcock, S. *Chem. Phys. Lett.* **1999**, *299*, 260.

(5) Bai, X. D.; Yu, J.; Liu, S.; Wang, E. G. *Chem. Phys. Lett.* **2000**, *325*, 485.

(6) Tang, C. C.; Bando, Y.; Golberg, D.; Ding, X. X.; Qi, S. R. *J. Phys. Chem. B* **2003**, *107*, 6539.

(7) Ma, R. Z.; Bando, Y.; Sato, T. *Chem. Phys. Lett.* **2001**, *350*, 1.

(8) Bando, Y.; Ogawa, K.; Golberg, D. *Chem. Phys. Lett.* **2001**, *347*, 349.

(9) Ma, R. Z.; Bando, Y.; Sato, T.; Kurashima, K. *Chem Mater.* **2001**, *13*, 2965.

(10) Narita, I.; Oku, T. *Diamond Relat. Mater.* **2003**, *12*, 1146.

(11) Gao, X. P.; Qin, X.; Wu, F.; Liu, H.; Lan, Y.; Fan, S. S.; Yuan, H. T.; Song, D. Y.; Shen, P. W. *Chem. Phys.* Lett. **2000**, *327*, 271.

(12) Shaijumon, M. M.; Ramaprabhu, S. *Chem. Phys. Lett.* **2003**, *374*, 513.

(13) Schlapbach, L.; Züttel, A. *Nature* **2001**, *414*, 353.

(14) Liu, C.; Fan, Y. Y.; Liu, M.; Cong, H. T.; Cheng, H. M.; Dresselhaus, M. S. *Science* **1999**, *286*, 1127.

(15) Pinkerton, F. E.; Wicke, B. G.; Olk, C. H.; Tibbetts, G. G.; Meisner, G. P.; Meyer, M. S.; Herbst, J. F. *J. Phys. Chem. B* **2000**, *104*, 9460.

(16) Hirscher, M.; Becher, M.; Haluska, M.; Quintel, A.; Skakalova, V.; Choi, Y. M.; Dettlaff-Weglikowska, U.; Roth, S.; Stepanek, I.; Bernier, P.; Leonhardt, A.; Fink, J. *J. Alloys Compd.* **2002**, *330*, 654.

(17) Ma, R. Z.; Bando, Y.; Zhu, H. W.; Sato, T.; Xu, C. L.; Wu, D. H. *J. Am. Chem. Soc.* **2002**, *124*, 7672.

(18) Tang, C. C.; Bando, Y.; Ding, X. X.; Qi, S. R.; Golberg, D. *J. Am. Chem. Soc.* **2002**, *124*, 14550.

(19) Jhi, S. H.; Kwon, Y. K. *Phys. Rev. B* **2004**, *69*, 245407.

(20) Wu, X. J.; Yang J. L.; Hou, J. G.; Zhu, Q. S. *J. Chem. Phys.* **2004**, *121*, 8481.

(21) Nützenadel, C.; Züttel, A.; Chartouni, D.; Schlapbach, L. *Electrochem. Solid-State Lett.* **1999**, *2*, 30.

(22) Qin, X.; Gao, X. P.; Liu, H.; Yuan, H. T.; Yan, D. Y.; Gong, W. L.; Song, D. Y. *Electrochem. Solid-State Lett.* **2000**, *3*, 532.

(23) Rajalakshmi, N.; Dhathathreyan, K. S.; Govinraraj, A.; Satishkumar, B. C. *Electrochim. Acta* **2000**, *45*, 4511.

(24) Lombardi, I.; Bestetti, M.; Mazzocchia, C.; Cavallotti, P. L.; Ducati, U. *Electrochem. Solid-State Lett.* **2004**, *7*, A115.

(25) Jurewicz, K.; Frackowiak, E.; Beguin, F. *Electrochem. Solid-State Lett.* **2001**, *4*, A27.

(26) Skowronski, J. M.; Scharff, P.; Pfander, N.; Cui, S. *Adv Mater.* **2003**, *15*, 55.

(27) Jurewicz, K.; Frackowiak, E.; Beguin, F. *Appl. Phys. A* **2004**, *78*, 981.

(28) Tang, C. C.; Bando, Y.; Sato, T. *Chem. Phys. Lett.* **2002**, *362*, 185.

(29) Yan, X. Q.; Gao, X. P.; Li, Y.; Liu, Z. Q.; Wu, F.; Shen, Y. T.; Song, D. Y. *Chem. Phys. Lett.* **2003**, *372*, 336.

(30) Gao, X. P.; Liu, J.; Ye, S. H.; Song, D. Y.; Zhang, Y. S. *J. Alloys Compd.* **1997**, *253−254*, 515.

(31) Wu, X. J.; Yang, J. L.; Hou, J. G.; Zhu Q. S. *Phys Rev. B* **2004**, *69*, 153411.

(32) Lukaszewski, M.; Kusmierczyk, K.; Kotowski, J.; Siwek, H.; Czerwinski, A. *J. Solid State Electrochem.* **2003**, *7*, 69.

(33) Czerwinski, A.; Kiersztyn, I.; Grden, M. *J. Solid State Electrochem.* **2003**, *7*, 321.

(34) Gao, X. P.; Lan, Y.; Pan, G. L.; Wu, F.; Qu, J. Q.; Song, D. Y.; Shen, P. W. *Electrochem. Solid-State Lett.* **2001**, *4*, A173.

(35) Yoo, E.; Gao, L.; Komatsu, T.; Yagai, N.; Arai, K.; Yamazaki, T.; Matsuishi, K.; Matsumoto, T.; Nakamura, J. *J. Phys. Chem. B* **2004**, *108*, 18903.